Modelling and Simulation of the Transient Electromagnetic Behavior of High Power Bus Bars

Peter Böhm, Gerhard Wachutka, Ronald H. W. Hoppe

Angaben zur Veröffentlichung / Publication details:

Böhm, Peter, Gerhard Wachutka, and Ronald H. W. Hoppe. 2002. "Modelling and Simulation of the Transient Electromagnetic Behavior of High Power Bus Bars." *Lecture Notes in Computational Science and Engineering* 21: 385–92. https://doi.org/10.1007/978-3-642-55919-8_42.

Modelling and Simulation of the Transient Electromagnetic Behavior of High Power Bus Bars

P. Böhm[1], G. Wachutka[1], and R.H.W. Hoppe[2]

[1] Institute for Physics of Electrotechnology, Munich University of Technology, D-80290 Munich, Germany
[2] Institute of Mathematics, University of Augsburg, D-86159 Augsburg, Germany

Abstract. An extended concept for the characterization of the electromagnetic behavior of high power bus bars in high power semiconductor modules is presented. Based on a three-dimensional transient finite element analysis of the electromagnetic field under realistic switching conditions, the eigendynamics of interconnects is evaluated. It is demonstrated that the investigation of distributed parasitic effects caused by short switching times and steep current or voltage ramps complements the common circuit analysis approach. The different modelling and simulation techniques in use are discussed focusing on specific numerical requirements. The capabilities of the method are demonstrated by some illustrative numerical examples.

1 Introduction

The optimization of high power components based on fast switching power semiconductor devices requires an integral approach that takes into account the overall performance of a module including the system-specific parasitic effects. With increasing switching frequencies and ever shorter pulse width, the eigendynamics inherent in the system becomes relevant and, hence, has to be included in the system analysis. Along with electrothermal aspects, the transient electromagnetic behavior of the interconnects can no longer be neglected. Therefore, the characterization of a complex, multiply contacted bus bar, or a system of bus bars, respectively, has to include the concept of time-dependent inductance. Induced overvoltage peaks, not only resulting from the time-derivative of the terminal current but also reflecting the time-dependence of the inductance, have to be considered as they can damage the attached semiconductor devices. Inhomogeneous current distributions in the interconnects do not only cause non-negligible electrothermal heating, but they can also lead to malfunction of large-scaled semiconductor switches which require a most homogeneous current distribution along the contacts. Moreover, the switching behavior may no longer be governed by the turn-on time of the semiconductor switches in use, but rather by the turn-on delay caused by the inductances of the bus bars.

2 Conventional Approach

Commonly the characterization and description of the electromagnetic behavior of high power bus bar structures is restricted to the determination of the integral quantities resistance, terminal currents and terminal voltages, and the extraction of the static inductance matrix of self- and mutual inductance coefficients. Apart from the widely employed heuristic approaches [1], there exists a well-established numerical method for inductance extraction, namely the Partial-Element-Equivalent-Circuit-Method (PEEC) [2]. This method is based on the calculation of the partial inductances by evaluating Neumann's formula.

$$L_{f_{ij}} = \frac{\mu}{4\pi} \oint_{C_i} \oint_{C_j} \frac{d\boldsymbol{l}_i d\boldsymbol{l}_j}{r_{ij}} \tag{1}$$

$L_{f_{ij}}$ denotes an inductance matrix element, the index f indicates that current filaments are considered, $r_{ij} = |\boldsymbol{r}_i - \boldsymbol{r}_j|$ and $d\boldsymbol{l}_i$ is an element of conductor i. For the evaluation of (1), the interconnects are partitioned into brick-shaped parts where each brick is associated with a current filament [3]. Therefore the PEEC-method is quite restricted with respect to the geometrical shape.

Besides other integration techniques are used to evaluate this formula, for example by multipole expansion [4] or Monte Carlo integration [5].

3 Extended FEM Based Approach

However, all above-mentioned methods are restricted to the quasi-magneto–static or the time-harmonic case. But for the analysis of the fast transient behavior of interconnects and in view of the wide variety of associated target functionals, a detailed understanding of the electromagnetic fields inside and outside the interconnects is essential. For this purpose it is more appropriate to stay in the time domain and not to change to the frequency domain by Fourier analysis.

We have already presented a methodology for the analysis of the transient electromagnetic behavior of multiply contacted interconnects based on the "field diffusion approximation" [6,7]. This methodology requires an efficient solver for the associated electric and magnetic potentials. To this end, we extended the finite element simulator SESES [8] by an electromagnetic kernel based on the $\boldsymbol{A}, V$-$\boldsymbol{A}$ formalism [9] which stands for solving the magnetic vector and electric scalar potentials $(\boldsymbol{A}, \varphi)$ inside the conducting region(s) and $\boldsymbol{A}$ in the nonconducting region(s).

The finite element simulator SESES provides a number of features essential for the simulation of the transient electromagnetic behavior of interconnects. Besides a mesh generator based on hexahedral isoparametric elements, which are very well suited to the shape of multiply banded and cutted plates,

the simulator features effective refinement techniques in space and time, e. g. a recursive adaptation of the mesh [10]. This is indispensable for economizing the number of elements, in order to save computing time while keeping the discretization error small at the same time.

These capabilities are demonstrated by a simple two-dimensional example, namely a rectangular conductor embedded in a non-conducting environment (Fig. 1). A current ramp is used as bias condition. As one of the features of the simulator, the efficiency of a global refinement strategy is demonstrated in Fig. 2. We find that the mesh is refined at the corners of the conductive rectangle, where the current density has its maximum inhomogeneity due to the skin effect, while it remains nearly unchanged elsewhere. As we want to solve the problem in the time domain, the number of time steps of transient simulations has to be minimized by an efficient time-stepping scheme as illustrated in Fig. 3. Starting with a time step of $1ns$, for instance, the program soon reaches a default value of $100ns$. The reduced time step at about $t = 3.0 \cdot 10^{-7}s$ is caused by a coincidence of the prescribed, user defined maximum time step and the automatically chosen time step.

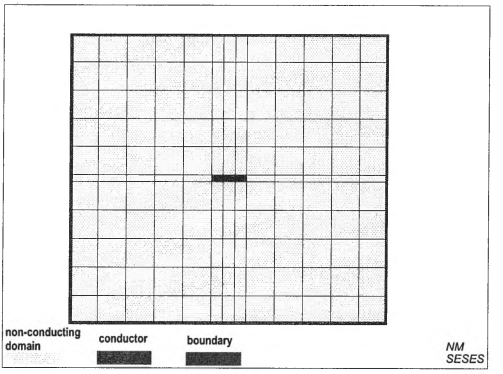

Fig. 1. Exemplary problem: Simulation domain and initial mesh of a two-dimensional rectangular conductor embedded in a non-conducting environment

4 Examples

In an illustrative example, the above-described computational functionality of the simulator is demonstrated by the simulation of a three-dimensional skin effect problem. Fig. 4 shows the finite element grid for the computation of a conducting bar in a non-conducting environment. For symmetry reasons, only one fourth of the bus bar is simulated. According to most of the cases encountered in practice, the skin depth is much less than the dimension of

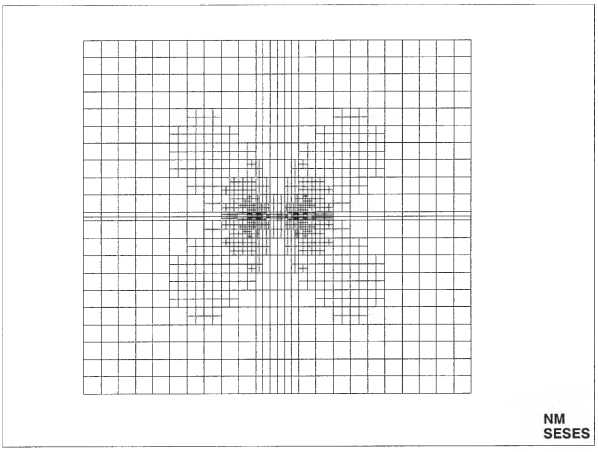

Fig. 2. Final mesh as obtained by global refinement strategy (number of elements: 1400)

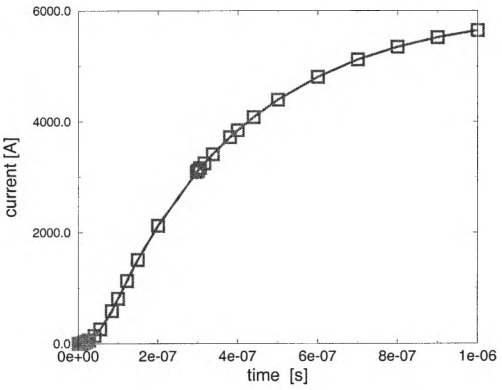

Fig. 3. Simulated time-dependent current flow demonstrating the capabilities of SESES with respect to time adaptivity

the investigated bus bar structure. Therefore, we start with a coarse grid for both the conducting and the non-conducting region. Then a user defined thin "surface layer" of elements with a thickness in the range of the skin depths is added underneath the conductor surface. This layer is subsequently refined and adapted to the surrounding grid by automatic adaptive mesh refinement. Elements with a bad aspect ratio in the non-conducting area are of minor influence, whereas a non-adapted grid in the conducting region, which would lead to an ill-conditioned discretized problem, is avoided by the automatic

mesh refinement. The mesh is flexible enough to resolve the skin effect, but also to reduce the number of elements to a minimum.

Fig. 4 and Fig. 5 show the current distribution inside the conducting bar at different time steps. A voltage ramp with a pulse rise-time of $0.1\mu s$ is used as bias condition. At $t = 10\mu s$ the current distribution is still dominated by the skin effect, which is clearly resolved. The current density in the bulk is by some orders of magnitude smaller than the current density in the skin layer. Even at $t = 1000\mu s$, the skin effect is still noticeable and the current distribution reaches a steady state not before $t = 10ms$.

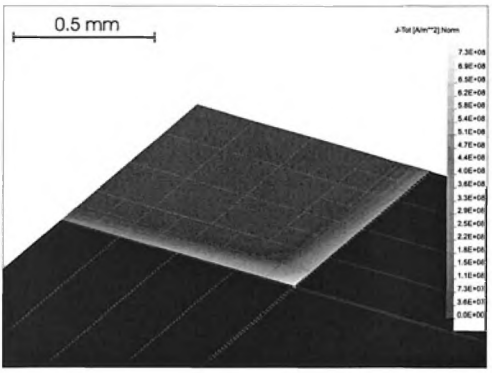

Fig. 4. Simulated current distribution at $t = 10\mu s$ for a 3D skin effect problem of a conducting bar in a non-conducting environment

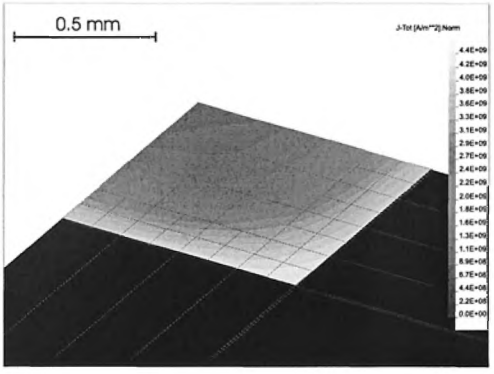

Fig. 5. Simulated current distribution at $t = 1000\mu s$ for a 3D skin effect problem

As a further example, a simplified but typical high power bus bar structure was analyzed for different geometrical modifications (Fig. 6). This bus bar is made of copper plates with a thickness of $1\,mm$ and a length of $14\,cm$. The plate is connected at the left and right side faces to a voltage source with a rise-time of $100ns$ and a constant value of $U = 0.01V$ afterwards. Special attention is paid to the transient states, where the skin effect is the dominant factor, by comparing them with the static state.

At $t = 1\mu s$, ten times later than the end of turn-on, the current distribution is still dominated by the skin effect which displaces the current to the outer corners of the structure (Fig. 6). For comparison, Fig. 7 shows the quasistatic current distribution which is attained at $t \approx 1000\mu s$ and plotted for $t = 1.11s$. The terminal current passing the contact electrodes shows, as a function of time, a behavior similar to that of a simple RL network element.

In Fig. 8, the time-dependent inductance is plotted. As the bus bars considered here have just two contacts, the terminal behavior of the structure is characterized by its self-inductance, which increases for $0 \leq t \leq 1000\mu s$ until the so called inner self-inductance has fully built-up. A structure possessing a L-shaped structure (Fig. 6) causes a partial compensation of the magnetic field between the L-structure, which results in a reduced inductance in comparison with a plain structure (dotted line in Fig. 8).

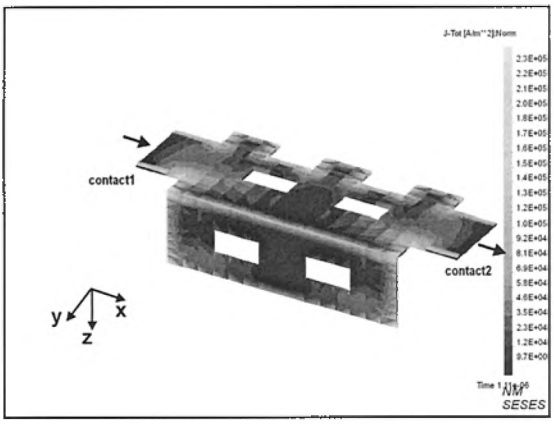

Fig. 6. Simulated current distribution at $t = 1.11\mu s$ for a simplified bus bar structure

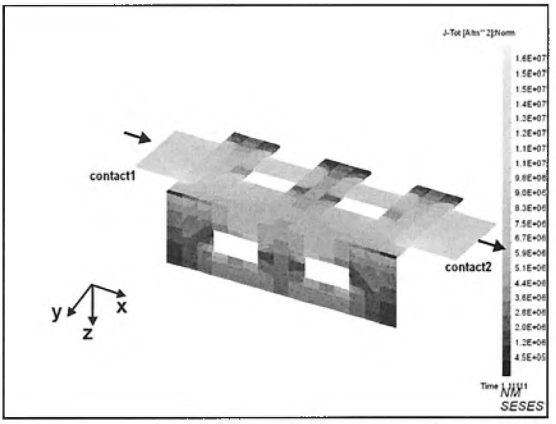

Fig. 7. Stationary current distribution at $t = 1.11s$

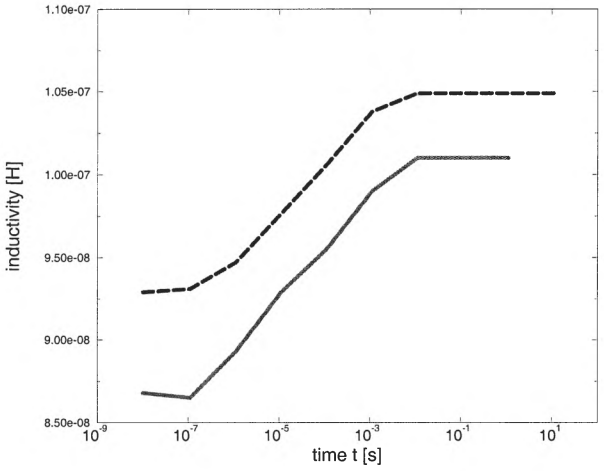

Fig. 8. Simulated time-dependent inductance of the interconnect for different geometries

5 Conclusion

The finite element simulator SESES allows the numerical analysis of the transient electromagnetic behavior of interconnects under realistic switching conditions. Equipped with the terminal characteristics and time-dependent impedence coefficients extracted from the transient electric and magnetic fields and with a view to shape optimization, we are able to define target functionals to assess the quality of a given interconnect set-up with respect to the uniformity of current flow, switching time delay, overvoltage and overheating limitations and related quantities of interest. In addition, our methodological concept provides a future perspective of extracting a set of time-dependent inductance coefficients required as input for circuit-level full system simulations of high power modules.

References

1. Skibinski, G.L., Divan, D.M.: Design Methodology & Modeling of Low Inductance Planar Bus Structures. Proc. of EPE, Brigthon, Great Britain, (1993) 98–105
2. Ruehli, A.E.: Inductance Calculation in a Complex Integrated Circuit Environment. IBM-Journal of Research and Development (1972) 470–481
3. Clavel, E., Schanen, J.L., Roudet, J.: Electromagnetic Modeling of a Power Module Case. IEEE EUROEM, (1994)
4. Kamon, M., Tsuk, M.J., White, J.: Fasthenry: A multipole-accelerated 3-d inductance extraction program. IEEE Trans. On Microwave Theory and Techniques **42** (1994) 1750–1758
5. Leonhardt, G., Fichtner, W.: Acceleration of Inductance Extraction by Means of the Monte Carlo Method. Proc. of MSM, San Juan, Puerto Rico (1999) 147–150
6. Böhm, P., Falck, E., Sigg, J., Wachutka, G.: Continuous Field Analysis of Distributed Parasitic Effects by Interconnects in High Power Semiconductor Modules. Proc. of SISPAD, Leuven, Belgium (1998) 340–343
7. Böhm, P., Wachutka, G.: Transient Electromagnetic Behavior of Multiply Contacted Interconnects. Proc. of MSM, San Juan, Puerto Rico (1999) 301–304
8. NM-SESES User Manual 5.0. Published by NM Numerical Modelling GmbH, Winterthur, Switzerland (1998)
9. Bíró, O., Preis, K.: On the Use of the Magnetic Vector Potential in the Finite Element Analysis of Three-Dimensional Eddy Currents. IEEE Trans. Mag. **25** (1989) 3145–3159
10. Korvink, J. G.: An Implementation of the Adaptive Finite Element Method for Semiconductor Sensor Simulation. Dissertation 10143, ETH Zürich (1993)